

Neutron powder diffraction study of $\text{TbBaCo}_{2-x}\text{Fe}_x\text{O}_{5+\gamma}$ layered oxides

D.D. Khalyavin,^{a,b,*} A.M. Balagurov,^b A.I. Beskrovnyi,^b I.O. Troyanchuk,^a
A.P. Sazonov,^a E.V. Tsipis,^c and V.V. Kharton^c

^aInstitute of Solid State and Semiconductors Physics, National Academy of Sciences, P. Brovka str. 17, 220072 Minsk, Belarus

^bFrank Laboratory of Neutron Physics, JINR, 141980 Dubna, Russia

^cDepartment of Ceramics and Glass Engineering, University of Aveiro, CICECO, Aveiro 3810-193, Portugal

Received 18 April 2003; received in revised form 16 August 2003; accepted 11 February 2004

Abstract

The crystal and magnetic structures of layered perovskites $\text{TbBaCo}_{2-x}\text{Fe}_x\text{O}_{5+\gamma}$ ($0.08 \leq x \leq 0.24$) were studied by neutron powder diffraction. Increasing iron concentration up to the x values higher than 0.10 leads to the orthorhombic \rightarrow tetragonal phase transition resulting from the transformation of $2 \times 1 \times 1$ -type superstructure, formed due to ordering of extra oxygen incorporated into the vacant sites in $[\text{TbO}_\gamma]$ layers, into $3 \times 3 \times 1$ superlattice. The concentration ranges, where the orthorhombic and tetragonal lattices exist, are separated with a narrow two-phase domain. For the tetragonal phases with $3 \times 3 \times 1$ superstructure (space group $P4/mmm$), the Co/Fe ions are antiferromagnetically coupled, forming G-type spin-ordered configuration. The Co^{3+} cations located in square-pyramidal sites adopt intermediate spin state, whilst a relatively small magnetic moment of Co^{3+} ions in the octahedral sublattice indicates that a minor fraction of cobalt is in the low-spin state.

© 2004 Elsevier Inc. All rights reserved.

PACS: 75.50,82.80.E

Keywords: Layered perovskite; Magnetic structure; Spin state; Oxygen vacancies ordering; Neutron diffraction

Unusual magnetic and transport properties have been reported for layered orthocobaltites of $\text{LnBaCo}_2\text{O}_{5+\gamma}$ family, where Ln is lanthanide or Y, and γ is the oxygen nonstoichiometry varying in a wide range from 0 to 0.7 [1–4]. These oxides exhibit, in particular, a variety of magnetic and structural phase transitions accompanied by the charge- and orbital-ordering phenomena, induced by the oxygen content variations [5–7]. Crystal lattice of such compounds, which is closely related to the YBaFeCuO_5 -type structure and can be easily derived from perovskite, represents a consequence of $[\text{CoO}_2]$ – $[\text{BaO}]$ – $[\text{CoO}_2]$ – $[\text{LnO}_\gamma]$ layers stacked along c -axis. When the concentration of oxygen vacancies located in the $[\text{LnO}_\gamma]$ layers is maximum ($\gamma = 0$), the crystal structure is

isostructural to YBaFeCuO_5 , with a $1 \times 1 \times 2$ superstructure due to the ordering of Ln^{3+} and Ba^{2+} ions occupying the corresponding layers; all cobalt cations are located within square pyramids with five-fold coordination. As γ increases, extra oxygen ions occupy vacant sites in $[\text{LnO}_\gamma]$ layers, thus providing octahedral environment for a part of Co ions. Two types of superstructure, $2 \times 1 \times 1$ ($0.5 \leq \gamma \leq 0.52$) and $3 \times 3 \times 1$ ($0.25 \leq \gamma \leq 0.44$), may be formed due to ordering of the extra oxygen [4, 8]; this corresponds to orthorhombic (O) and tetragonal (T) symmetry of the crystal structure, respectively. In a narrow concentration range ($0.44 < \gamma < 0.5$), the orthorhombic and tetragonal phases co-exist [8]. The structure and physical properties of the O-type $\text{LnBaCo}_2\text{O}_{5.5}$ perovskites with $2 \times 1 \times 1$ superstructure are known in Refs. [4,9,10]. In this case, the extra oxygen ions and vacancies are located in the chains along a -axis within $[\text{LnO}_{0.5}]$ layers; the planes formed by CoO_5 pyramids and CoO_6 octahedra alternate along the b -axis. On the contrary, literature data on the structure

*Corresponding author. Institute of Solid State and Semiconductors Physics, National Academy of Sciences, P. Brovka str. 17, 220072 Minsk, Belarus. Fax: +375-0172-84-08-88.

E-mail address: khalyav@ifttp.bas-net.by (D.D. Khalyavin).

of tetragonal orthocobaltites with $3 \times 3 \times 1$ superlattice are scarce.

Previous work [11] reported the O–T transition induced by iron doping in the $\text{TbBaCo}_{2-x}\text{Fe}_x\text{O}_{5+\gamma}$ system. For these perovskites, the lattice is orthorhombic at $x \leq 0.10$ and tetragonal when $x \geq 0.12$; the material with $x = 0.11$ was found to contain both phases [11]. Mössbauer spectroscopy data showed that Fe^{3+} ions occupy three (one high- and two low-symmetry) or two (low-symmetry) sites for the T- and O-type structure, respectively [11]. In the latter case, both iron positions are 5-coordinated; first of them corresponds to the regular square-pyramidal site in the structure of the $\text{LnBaCo}_2\text{O}_{5.5}$, while the second pyramidal position results from the octahedral sites when one oxygen ion is removed from the $[\text{TbO}_{0.5}]$ layer. Due to this, iron substitution leads to decreasing oxygen content, as confirmed by thermogravimetric analysis (TGA) [11].

The concentration-dependent transformation from orthorhombic into tetragonal lattice of $\text{TbBaCo}_{2-x}\text{Fe}_x\text{O}_{5+\gamma}$ at $x \approx 0.1$ might result either from disordering of the excess oxygen in $[\text{TbO}_\gamma]$ layers (order–disorder transition), or from the superstructure change due to decreasing oxygen content (order–order transition). Three different positions of iron ions in the tetragonal phases ($x \geq 0.12$) suggest that the second mechanism is more likely. In this case, the highly symmetric position corresponds to the octahedrally coordinated sites; the two low-symmetry positions relate to Fe cations in square-pyramidal sites, formed as for the orthorhombic structure. In case of the order–disorder transition, only one low-symmetry position of the iron ions should be expected. However, additional structural studies are necessary to clarify exact mechanism of this transformation. In the present work, the crystal and magnetic structures of the $\text{TbBaCo}_{2-x}\text{Fe}_x\text{O}_{5+\gamma}$ perovskites were determined using the neutron powder diffraction method.

The polycrystalline samples of $\text{TbBaCo}_{2-x}\text{Fe}_x\text{O}_{5+\gamma}$ ($x = 0.08–0.15$ with step 0.01, and $x = 0.24$) were prepared by a standard ceramic route from the stoichiometric amounts of Tb_2O_3 , Co_3O_4 , Fe_2O_3 and BaCO_3 . After pressing and pre-firing at 1173 K, the pellets were reground and annealed in air for 10 h at different temperatures, varying in the range 1323–1473 K. The sample of $\text{TbBaCo}_{1.76}\text{Fe}_{0.24}\text{O}_{5+\gamma}$ was cooled down to room temperature with a rate of 100 K/h; for other compositions cooling rate varied from 2 to 250 K/h. Neutron powder diffraction experiments were carried out at the IBR-2 pulsed reactor of the Joint Institute for Nuclear Research (JINR, Russia), and at the SINQ spallation source of the Paul Scherrer Institute (PSI, Switzerland). The crystal structures were determined from the data taken using the high-resolution Fourier diffractometer HRFD and neutron diffractometer DN2 (JINR). Data on the magnetic

ordering and possible superstructures were obtained using the DMC powder diffractometer (PSI), situated at a supermirror coated guide for cold neutrons at SINQ ($\lambda = 4.2 \text{ \AA}$).

As mentioned above, X-ray diffraction (XRD) data on $\text{TbBaCo}_{2-x}\text{Fe}_x\text{O}_{5+\gamma}$ system [11] showed an existence of narrow two-phase domain separating the concentration ranges where the O- and T-type phases are formed. As an example, Fig. 1 presents the time-of-flight (TOF) neutron diffraction spectrum of $\text{TbBaCo}_{1.86}\text{Fe}_{0.14}\text{O}_{5+\gamma}$, collected at room temperature. The reflections of both orthorhombic (space group $Pmmm$) and tetragonal (S.G. $P4/mmm$) lattices can be clearly distinguished; Rietveld refinement gives the O:T phase concentration ratio of about 61:39. The neutron diffraction studies of $\text{TbBaCo}_{2-x}\text{Fe}_x\text{O}_{5+\gamma}$, having compositions around the structural transition ($x \sim 0.1$) and prepared in different conditions, revealed that the range of x values corresponding to the two-phase domain is essentially independent of synthesis temperature, but can be slightly changed if varying the rate of cooling after sintering. When cooling rate decreases from 250 to 2 K/h, the two-phase domain shifts from $0.09 < x < 0.12$ to $0.12 < x < 0.14$. However, when the materials with different iron content are prepared under the same conditions, formation of the phase mixture in a narrow range of x ($\Delta x \approx 0.02–0.03$) is observed in all cases. This confirms an existence of miscibility gap between the O and T phases in the $\text{TbBaCo}_{2-x}\text{Fe}_x\text{O}_{5+\gamma}$ system.

Analysis of the neutron diffraction spectrum of tetragonal $\text{TbBaCo}_{1.76}\text{Fe}_{0.24}\text{O}_{5+\gamma}$, collected above

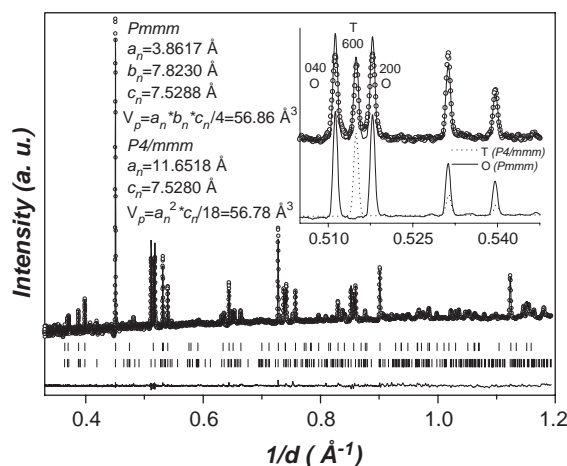


Fig. 1. Neutron diffraction spectrum of the two-phase $\text{TbBaCo}_{1.86}\text{Fe}_{0.14}\text{O}_{5+\gamma}$ at 300 K (HRFD diffractometer). Experimental, calculated and difference patterns are shown; the difference curve is normalized for the mean square deviation. Vertical lines indicate the positions of Bragg peaks for tetragonal (top) and orthorhombic (bottom) phases. Inset shows the (200) multiplet in the cubic approximation. The reflections of the orthorhombic and tetragonal phases are indexed in $a_n \approx a_p$, $b_n \approx 2a_p$, $c_n \approx 2a_p$ and $a_n \approx 3a_p$, $c_n \approx 2a_p$ (a_p —the perovskite unit cell constant) unit cells respectively.

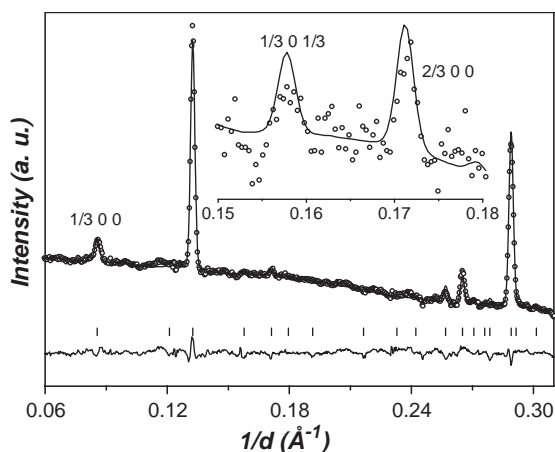


Fig. 2. Observed (DMC, $\lambda = 4.2 \text{ \AA}$), calculated, and difference patterns of $\text{TbBaCo}_{1.76}\text{Fe}_{0.24}\text{O}_{5+\gamma}$ at 300 K.

the magnetic ordering point, shows a presence of superstructure reflections corresponding to a tripled a parameter of the primitive perovskite unit cell, (Fig. 2). Again, this is in excellent agreement with assumption [11] concerning $3 \times 3 \times 1$ superlattice type in the tetragonal $\text{TbBaCo}_{2-x}\text{Fe}_x\text{O}_{5+\gamma}$. One can therefore conclude that, as for other $\text{LnBaCo}_{2-x}\text{Fe}_x\text{O}_{5+\gamma}$ perovskites changes due to the change of oxygen-vacancy ordering type when the iron content increases. If compared to other possible models of $3 \times 3 \times 1$ superstructure [8], the best agreement with experiment was found for the model shown in Fig. 3. Neglecting oxygen content fluctuations, the value of γ for this superstructure model is 0.44. There are, hence, 4/9 octahedral and 5/9 square-pyramidal positions for Co/Fe ions per unit formula (Fig. 3a). The distribution of oxygen anions forming a $3 \times 3 \times 1$ superstructure in $[\text{TbO}_{0.44}]$ layers is shown in Fig. 3b. The refined TOF neutron diffraction pattern of $\text{TbBaCo}_{1.76}\text{Fe}_{0.24}\text{O}_{5+\gamma}$ is shown in Fig. 4; Table 1 lists the structure refinement results.

It should be mentioned that $\text{TbBaCo}_{1.76}\text{Fe}_{0.24}\text{O}_{5+\gamma}$ perovskite exhibits no spontaneous magnetization in the temperature range 4.2–300 K, whereas the Mössbauer spectroscopy shows an appearance of the hyperfine splitting below $T_N = 270 \text{ K}$ [11]. This indicates anti-ferromagnetic ordering of the magnetic moments of cobalt and iron ions below T_N . Indeed, additional reflections appear in the neutron diffraction spectra at $T < T_N$ (Fig. 5). Calculations of the magnetic structure using a model, where each Co/Fe ion is antiferromagnetically coupled to its neighbors along all three directions (G-type ordering), gives reasonably good agreement factors ($R_{\text{nuc}} = 3.32\%$, $R_{\text{mag}} = 4.04\%$). The difference in the magnetic moment values for Co/Fe ions, occupying octahedral and pyramidal sites, leads to a nonzero magnetic structure factor for 211 reflection. At $T = 25 \text{ K}$, the refined magnetic moments lying in

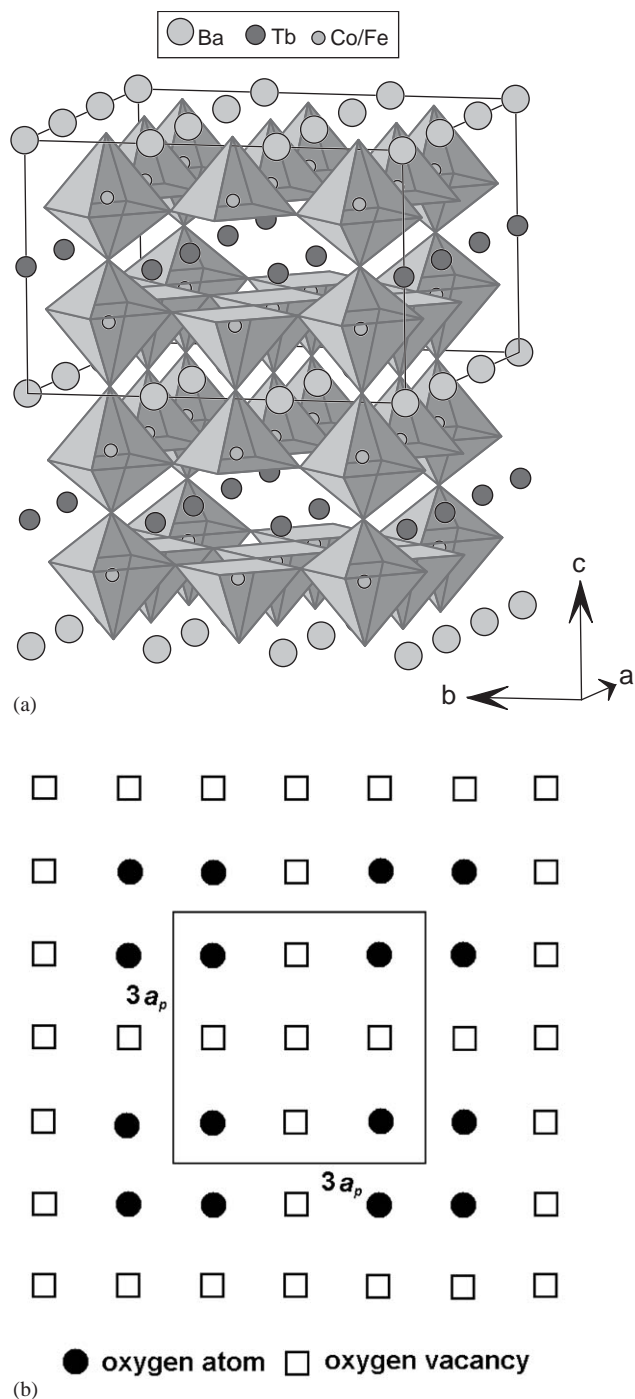


Fig. 3. Schematic representation of the crystal structure of tetragonal $\text{TbBaCo}_{2-x}\text{Fe}_x\text{O}_{5+\gamma}$ with $3 \times 3 \times 1$ superstructure (a). The distribution of oxygen anions forming a $3 \times 3 \times 1$ superstructure in $[\text{TbO}_{0.44}]$ layers (b).

(ab) plane are $\mu_{\text{pyr}} = 2.8(2)$ and $\mu_{\text{oct}} = 1.6(2) \mu_B$ per Co/Fe ion for the pyramidal and octahedral positions, respectively. No evidence for a long-range ordering of the magnetic moments of Tb^{3+} ions was detected at 25 K. Apparently, the ordering of the terbium sublattice occurs at lower temperatures, as for $\text{TbBaCo}_2\text{O}_5$

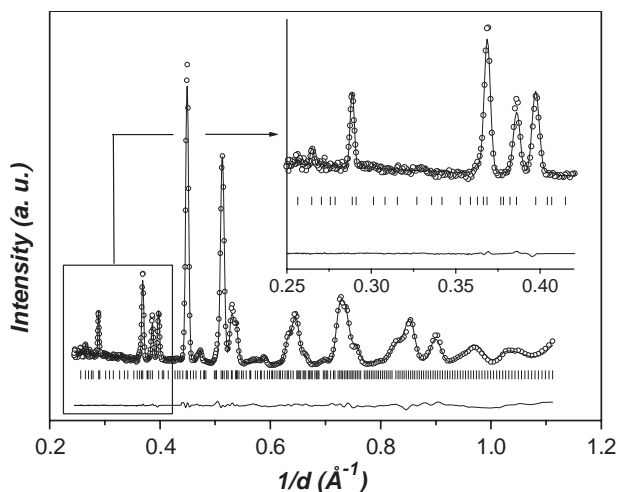


Fig. 4. Observed (DN2 diffractometer) and calculated (S.G. $P4/mmm$) intensity profile for $\text{TbBaCo}_{1.76}\text{Fe}_{0.24}\text{O}_{5+\gamma}$ at 300 K. Vertical lines indicate the positions for Bragg reflections. The difference plot is shown at the bottom.

Table 1

Crystallographic parameters of $\text{TbBaCo}_{1.76}\text{Fe}_{0.24}\text{O}_{5+\gamma}$, obtained by the Rietveld refinement of neutron diffraction data (DN2 diffractometer). Space group $P4/mmm$, $a_n = 11.6940(4)$ Å, $c_n = 7.5461(5)$ Å, $V = 1031.926(1)$ Å³, $Z = 18$, $R_p = 3.18\%$, $R_{wp} = 3.86\%$.

Atom	Wyck	x	y	z	B (Å ²)	Occupancy
Ba1	$1a$	0	0	0	0.60(3)	1
Ba2	$4j$	1/3	1/3	0	0.60(3)	1
Ba3	$4l$	2/3	0	0	0.60(3)	1
Tb1	$1b$	0	0	1/2	0.41(5)	1
Tb2	$4m$	2/3	0	1/2	0.41(5)	1
Tb3	$4k$	1/3	1/3	1/2	0.41(5)	1
Co1	$2h$	1/2	1/2	0.270(2)	0.77(9)	0.88
Fe1	$2h$	1/2	1/2	0.270(2)	0.77(9)	0.12
Co2	$8r$	1/6	1/6	0.239(2)	0.77(9)	0.88
Fe2	$8r$	1/6	1/6	0.239(2)	0.77(9)	0.12
Co3	$8t$	1/6	1/2	0.270(2)	0.77(9)	0.88
Fe3	$8t$	1/6	1/2	0.270(2)	0.77(9)	0.12
O1	$4j$	1/6	1/6	0	0.99(11)	1
O2	$4n$	1/6	1/2	0	0.99(11)	1
O3	$1c$	1/2	1/2	0	0.99(11)	1
O4	$16u$	1/6	1/3	0.300(3)	1.05(8)	1
O5	$8s$	1/6	0	0.300(3)	1.05(8)	1
O6	$4i$	0	1/2	0.300(3)	1.05(8)	1
O7	$8t$	1/3	1/2	0.300(3)	1.05(8)	1
O8	$4k$	1/6	1/6	1/2	1.30(12)	0.732(11)
O9	$4o$	1/2	1/6	1/2	1.30(12)	0.087(12)

perovskite where the corresponding T_N value is about 4 K [7].

Prior to discussing magnetic moment value and spin state of the cobalt ions, let us write the chemical formula and charge distribution in $\text{TbBaCo}_{1.76}\text{Fe}_{0.24}\text{O}_{5+\gamma}$. According to the Mössbauer spectroscopy [11], iron ions in this perovskite have 3⁺ oxidation state with high-spin electronic configuration ($t_{2g}^3 e_g^2 S = 5/2$). Taking into account TGA data [11] and structure refinement results

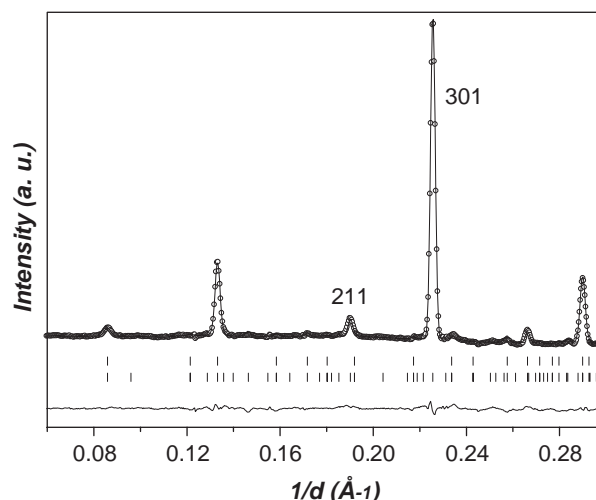


Fig. 5. Neutron diffraction pattern of $\text{TbBaCo}_{1.76}\text{Fe}_{0.24}\text{O}_{5+\gamma}$ at 25 K, collected on DMS ($\lambda = 4.2$ Å). Vertical lines indicate angular positions for the nuclear Bragg peaks (bottom) and for possible magnetic reflections (top). Lower part of the figure shows the difference plot. The magnetic reflections are indexed in the magnetic unit cell with $a_m = \sqrt{2}a_n$ and $c_m = c_n$.

(Table 1), the chemical formula can be written as $\text{TbBaCo}_{1.5}^{3+}\text{Co}_{0.26}^{2+}\text{Fe}_{0.24}^{3+}\text{O}_{5.37}$, with about 15% of cobalt ions existing in the divalent state. One can assume that the higher oxygen coordination should stabilize higher oxidation state of cobalt ions. In other words, Co^{2+} cations should be predominantly incorporated into crystallographic positions with a lower coordination (square-pyramidal), whilst the octahedral sites are mostly occupied by Co^{3+} . Mössbauer spectra [11] also showed that approximately 19% of iron ions are 6-coordinated. This means that Fe^{3+} occupies about 5% of the octahedral sites. The value of the magnetic moment $\mu_{\text{octr}} = 1.6(2) \mu_B$ per Co/Fe ion is relatively low for the case when Co^{3+} and Fe^{3+} exist in the intermediate ($t_{2g}^5 e_g^1 S = 1$) and high-spin states, respectively. Such a behavior results, most likely, from the existence of a minor fraction of six-fold coordinated Co^{3+} with low-spin electronic configuration ($t_{2g}^6 e_g^0 S = 0$). Assuming completely quenched orbital contribution to the magnetic moment of cobalt ($g \approx 2$), one can obtain approximately 72% and 23% of the octahedral positions occupied by Co^{3+} with the intermediate and low spin configurations, respectively. The value of $\mu_{\text{pyr}} = 2.8(2) \mu_B$ per Co/Fe ion can be easily explained considering the contributions of intermediate-spin Co^{3+} , high-spin Co^{2+} ($t_{2g}^5 e_g^2 S = 3/2$), and also high-spin Fe^{3+} .

The spin state of cobalt ions and magnetic structure for $Ln\text{BaCo}_2\text{O}_{5+\gamma}$ perovskites were discussed in numerous works [4–18]. In general, the attention was focused on only two distinct structural types with $\gamma \approx 0.5$ and $\gamma \approx 0$. For the former, several different models of the magnetic structure were proposed [12–18] and this

problem is still a matter of discussion. Nonetheless, one can make a definite conclusion regarding the spin state of cobalt ions in these compounds. Namely, various experimental data directly show that the square-pyramidal and octahedral positions are occupied by the intermediate- and low-spin Co^{3+} ions, respectively [9,14,15]. From this point of view, the electronic configuration of cobalt ions proposed in this work for $\text{TbBaCo}_{1.76}\text{Fe}_{0.24}\text{O}_{5.37}$ is quite logical. The high concentration of paramagnetic Co^{3+} in octahedral sites is apparently associated with the presence of iron cations, making the low-spin state of cobalt ions unstable in their local surrounding.

In the case when $\gamma = 0$, the experimental data certainly demonstrates that the magnetic moments of Co^{2+} and Co^{3+} ions, both adopting high spin state, are ordered antiferromagnetically, forming the G-type spin configuration [6,7,17,18]. The neutron diffraction study of $\text{NdBaCo}_2\text{O}_{5+\gamma}$ ($\gamma \approx 0.38$) recently reported by Burley et al. [18], revealed a coexistence of two phases with different oxygen contents, $\gamma = 0.29$ and $\gamma = 0.5$. Crystal structure of the former is derived from the structure of $\gamma = 0$ phase, with a random distribution of oxygen ions within $[\text{NdO}_\gamma]$ layers. Most likely, there exists a miscibility gap between two structural types with $\gamma = 0.5$ and $\gamma = 0$. Therefore, the $3 \times 3 \times 1$ superstructure, found in this work and in the cases of $\text{DyBaCo}_2\text{O}_{5+\gamma}$ and $\text{YBaCo}_2\text{O}_{5+\gamma}$, is only stable for compounds with small rare-earth ions. For the phase having $\gamma = 0.29$, the long-range G-type antiferromagnetic ordering was found at temperatures below 150 K. The value of the magnetic moment was interpreted assuming that the octahedral Co^{3+} ions adopt low spin state and the square-pyramidal $\text{Co}^{2+}/\text{Co}^{3+}$ are high spin, as for the $\gamma = 0$ materials. In the present case, accepting the model involving high-spin state for square-pyramidal Co^{3+} makes is necessary to assume that a part of the sample is not magnetically ordered. This would contradict to the low-temperature Mosbauer data [11].

In summary, the neutron diffraction studies of $\text{TbBaCo}_{2-x}\text{Fe}_x\text{O}_{5+\gamma}$ system showed that the orthorhombic-tetragonal phase transition results from changing the superstructure ($2 \times 1 \times 1 \rightarrow 3 \times 3 \times 1$), formed due to ordering of extra oxygen in $[\text{TbO}_\gamma]$ layers. The Co/Fe ions in tetragonal $\text{TbBaCo}_{1.76}\text{Fe}_{0.24}\text{O}_{5+\gamma}$ with $3 \times 3 \times 1$ superstructure type are antiferromagnetically coupled; the spin-ordering configuration is G-type. The refinement of magnetic peak intensities reveals that

Co^{3+} ions located in the square-pyramidal sites have intermediate-spin state, whereas a minor part of octahedrally coordinated Co^{3+} seems to adopt low-spin state.

This research was supported by the Swiss National Science Foundation (SCOPES program under the grant #7BYPJ65732), by the INTAS (grant #01-0278), by the Belarus Foundation for Basic Research (grant F02R-069), and by the FCT, Portugal (grant BD/6827/2001).

References

- [1] C. Martin, A. Maignan, D. Pelloquin, N. Nguyen, B. Raveau, *Appl. Phys. Lett.* 71 (1997) 1421–1423.
- [2] I.O. Troyanchuk, N.V. Kasper, D.D. Khalyavin, H. Szymczak, R. Szymczak, M. Baran, *Phys. Rev. Lett.* 80 (1998) 3380–3383.
- [3] I.O. Troyanchuk, N.V. Kasper, D.D. Khalyavin, H. Szymczak, R. Szymczak, M. Baran, *Phys. Rev. B* 58 (1998) 2418–2421.
- [4] A. Maignan, C. Martin, D. Pelloquin, N. Nguyen, B. Raveau, *J. Solid State Chem.* 142 (1999) 247–260.
- [5] T. Vogt, P.M. Woodward, P. Karen, B.A. Hunter, P. Henning, R. Moodenbaugh *Phys. Rev. Lett.* 84 (2000) 2969–2972.
- [6] E. Suard, F. Fauth, V. Caignaert, I. Mirebeau, G. Baldinozzi, *Phys. Rev. B* 61 (2000) 11871–11874.
- [7] F. Fauth, E. Suard, V. Caignaert, B. Domenges, I. Mirebeau, L. Keller, *Eur. Phys. J. B* 21 (2001) 163–174.
- [8] D. Akahoshi, Y. Ueda, *J. Solid State Chem.* 156 (2001) 355–363.
- [9] C. Frontera, J.L. Carcia-Munoz, A. Llobet, M.A.G. Aranda, *Phys. Rev. B* 65 (2002) 180,405–180,405-4.
- [10] H. Kusuya, A. Machida, Y. Moritomo, K. Kato, E. Nishibori, M. Takata, M. Sakata, A. Nakamura, *J. Phys. Soc. Japan* 70 (2001) 3577–3580.
- [11] M. Kopcewicz, D.D. Khalyavin, I.O. Troyanchuk, H. Szymczak, R. Szymczak, D.J. Logvinovich, E.N. Naumovich, *J. Appl. Phys.* 93 (2003) 479–486.
- [12] F. Fauth, E. Suard, V. Caignaert, I. Mirebeau, *Phys. Rev. B* 66 (2002) 184,421–184,421-5.
- [13] D.D. Khalyavin, I.O. Troyanchuk, N.V. Kasper, Q. Huang, J.W. Lynn, H. Szymczak, *J. Mater. Res.* 17 (2002) 838–843.
- [14] M. Soda, Y. Yasui, T. Fujita, M. Sato, K. Kakurai, *J. Phys. Soc. Japan* 72 (2003) 1729–1734.
- [15] A.A. Taskin, A.N. Lavrov, Y. Ando, *Phys. Rev. Lett.* 90 (2003) 227,201–227,201-4.
- [16] D.D. Khalyavin, S.N. Barilo, S.V. Shiryaev, G.L. Bychkov, I.O. Troyanchuk, A. Furrer, P. Allenspach, H. Szymczak, R. Szymczak, *Phys. Rev. B* 67 (2003) 214,421–214,421-5.
- [17] J.F. Mitchell, J.C. Burley, S. Short, *J. Appl. Phys.* 93 (2003) 7364–7366.
- [18] J.C. Burley, J.F. Mitchell, S. Short, D. Miller, Y. Tang, *J. Solid State Chem.* 170 (2003) 339–350.